Multi-Parametric Monitoring of Thermal Ablations using Rapid Chemical Shift Imaging

B. A. Taylor[1,2], A. M. Elliott[1], K-P. Hwang[1,3], J. D. Hazle[1], and R. J. Stafford[1]

[1]Imaging Physics, The University of Texas MD Anderson Cancer Center, Houston, Texas, United States, [2]The University of Texas Graduate School of Biomedical Sciences, Houston, Texas, United States, [3]Applied Science Laboratory, GE Healthcare, Waukesha, Wisconsin, United States

Introduction

MR has been shown to be quite effective in the localizing, planning, monitoring, and verification in thermal therapies. One actively-researched method of monitoring temperature is chemical shift imaging (CSI) since is can provide highly accurate and precise measurements of temperature in the presence of motion, lipid contamination, field drifts and susceptibility (1-3). An additional advantage is the extra parameters, such as R_2*, that are calculated when performing CSI. In this work, we utilize a published rapid chemical shift imaging (CSI) technique that monitors the PRF in addition to the R_2* and T_1-W amplitude of multiple proton-containing components (water, methylene, methyl, etc) at resolutions comparable to CPD techniques (1,2). We report the changes in these parameters as a function of temperature and compare them to changes predicted by Arrhenius rate analysis with hope that these parameters may help predict outcomes for thermal therapies.

Methods

Canine bone marrow, brain, kidney, liver and prostate tissue were treated with a water-cooled applicator housing a 980-nm laser fiber with a 1-cm diffusing tip powered by a 15 W diode laser source (BioTex Inc., Houston, TX) on a clinical MR scanners at 1.5T (Excite HD, GEHT, Waukesha, WI) and 3T (TwinSpeed Excite HD, GE Healthcare, Waukesha, WI). A fluoroptic temperature probe (M3300, Luxtron, Santa Clara, CA) was inserted in order to provide an absolute measurement of temperature. In each ablation, a multi-gradient echo (MGE) acquisition (1.5T: ETL=16 echoes; minimum TE (TE_0)=2.0 ms; ESP=3.2 ms; TR=69 ms; FA=30-40°; rBW=244 Hz/pixel, acquisition matrix=128x128; voxel volume=1.6x1.6x4.0 mm^3; 5 sec/image; parallel imaging acceleration factor=2. 3T: TE_0=2.1 ms; ESP=1.8 ms; rBW=325 Hz/pixel) was used. Echoes were acquired with identical polarity gradients separated by flyback rewinder gradients. ROIs (2 x 2 voxels) were chosen in areas that reached ablative temperatures (≥54 °C) with each pixel processed individually. Using the calculated temperature sensitivity coefficients from water (and bulk methylene PRF as an internal reference if present), the changes in the PRFs were converted to temperature changes and added to the baseline temperature provided by the fluoroptic temperature probe; thereby providing absolute temperature readings. The R_2* and signal amplitude (modeled using R_2* correction) values for water, bulk methylene, terminal methylene and methyl protons in bone, were measured as a function of absolute temperature. The slopes of lines were measured at different temperature ranges and compared using a two-tailed Student's t-test with equal variances (as determined by an F-Test). The R_2* values and T1-W amplitude as a function of temperature were compared with the Arrhenius rate model for thermal damage (3). A and E_a values were chosen to predict protein denaturation (A: 3.1 x 10^{98} s^{-1}, E_a: 6.3 x 10^5 J mol^{-1}) (4) and lipid bilayer disruption (A: 3.3 x 10^{47} s^{-1}, E_a: 2.9 x 10^5 J mol^{-1}) (5). In this study, Ω≥1 signified tissue damage and this threshold has been used to previous studies (6,7).

Results

The R_2* and signal amplitude of water and each lipid in bone marrow were plotted along with the Arrhenius rate estimate for irreversible tissue damage as a function of temperature in figure 1. The water R_2* plot (a) shows regions of linearity, but a marked slope polarity shift was observed at approximately 54 °C, which is where Ω≥1. The slope between 17 °C and 41 °C, 41 °C to 54 °C, and 54 °C and above were 0.239 ± 0.002 (s °C)$^{-1}$ (R^2=0.968), 0.130 ± 0.007 (s °C)$^{-1}$ (R^2=0.980). and -0.145 ± 0.003 (s °C)$^{-1}$ (R^2=0.917), respectively. Each of these slopes were statistically different from one another ($p<0.0001$). For bulk and terminal methylene there is an asymptotic decrease in R_2* until Ω approached unity. There was also a change in the methyl R_2* slope as Ω approached unity. In the amplitude measurements, a shift in the slope was observed in the water peak. At temperatures where Ω ≥1, the slope was -1.02 ± 0.02 %/°C (R^2=0.905). The temperature response reduced the bulk methylene, terminal methylene and methyl peaks by 75%, 88% and 80%, respectively, at the same temperature region. Figure 2 demonstrates what was typically seen in non-lipid tissue from the brain. Table 2 lists temperatures where the break points occurred according to Arrhenius rate model analysis along with the slopes between these temperatures. In all tissues except prostate, there was a statistically significant change in the R2* slope when damage is predicted to occur. This was more evident compared to the amplitude slopes. The slopes of PRF were at the range of -0.010 to -0.0097 ppm/°C. These were not observed to change at high temperatures.

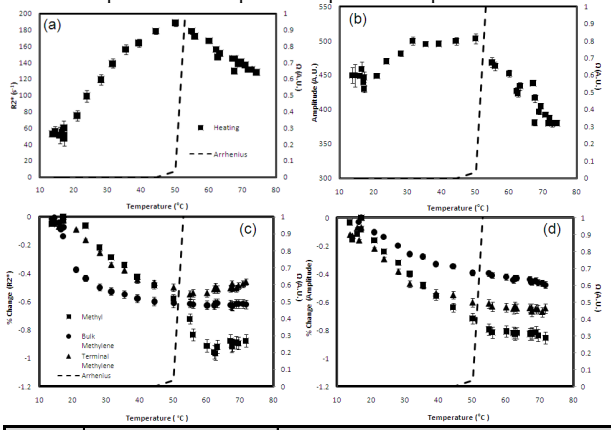

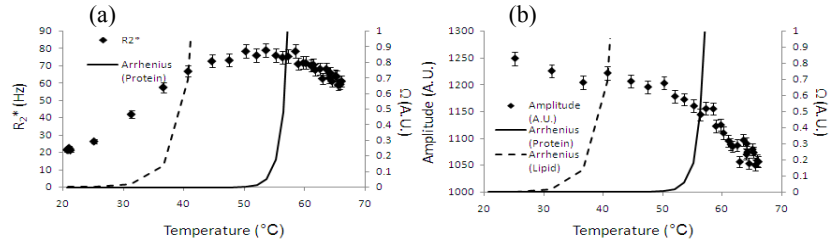

Figure 1 (Left): The water R_2* (a) and amplitude (b) as well as the lipid R_2* (c) and amplitude (d) of bone marrow at 3.0T. The dashed line in each plot represents the Arrhenius dose model calculation . Changes in the slope can be seen when the Arrhenius dose, Ω, approaches 1.0, which signifies damage to the tissue.

Figure 2 (Above): The water R_2* (a) and amplitude (b) of brain at 3.0T. As with the bone marrow, changes in slope can be seen when Ω approaches 1.0.

Tissue	Break Points (BP's) (°C)	R_2* Slope (%/°C)			Amplitude Slope (%/°C)		
		Body Temperature to 1st BP	1st BP to 2nd BP	Above 2nd BP	Body Temperature to 1st BP	1st BP to 2nd BP	Above 2nd BP
Brain	41.2±1.0, 57.1±1.2	6.3±0.2 (R^2=0.994)	0.5±0.2 (R^2=0.881)**	-4.3±0.6 (R2=0.792)**	-0.1±0.1 (R2=0.605)	-0.4±0.1 (R2=0.897)	-1.0±0.2 (R2=0.803)*
Prostate	41.3±0.7, 57.0±1.0	0.2±0.1 (R^2=0.930)	0.1±0.1 (R^2=0.328)	0.4±0.1 (R^2=0.565)	-0.2±0.2 (R2=0.907)	-0.4±0.1 (R2=0.970)	-0.5±0.1 (R2=0.944)
Liver	43.5±0.5, 52.2±0.4	1.0±0.2 (R2=0.981)	-0.1±0.1 (R2=0.130)**	1.2±0.1 (R2=0.894)**	-1.1±0.2 (R2=0.794)	-0.5±0.1 (R2=0.940)*	-0.9±0.2 (R2=0.924)*
Kidney	42.0±0.5, 57.0±0.4	1.0±0.4 (R2=0.670)	3.1±0.6 (R2=0.258)*	-1.0±0.4 (R2=0.717)**	-0.8±0.3 (R2=0.833)	-0.5±0.1 (R2=0.813)	-0.7±0.1 (R2=0.857)

Table 1: Temperature break points (Ω ≥1) with linear regression slopes above/below these points.(* $p<0.05$,** $p<0.001$ compared to slope before the break point)

Discussion

With this technique peak-specific R_2* and T_1-weighted amplitudes can be measured to provide an important opportunity to observe changes as a function of temperature. In this analysis we saw changes in linearity of the R_2* and amplitude signal during heating, similar to what has been observed in other tissues (8). However, using the temperature history, we've noted that the significant changes in the temperature dependence of these parameters for water and lipid in the range where the Arrhenius rate model predicts damage (4,5). This could be a useful tool for evaluating dosimetry models for thermal ablation. When Ω≥1, there was a consistent, sharp, measureable change in the slope of the R_2* of water versus temperature. Therefore, it appears that using the multiparametric spectral estimates provided by the high spatiotemporal resolution chemical shift imaging sequence during heating may return information on physical tissue changes taking place, such as conformational phase transitions of lipid bilayers and proteins, which directly influence the proton chemical macroenvironment and, thereby, relaxation as observed in R_2* mapping and T_1-W signal changes. These observations warrant further investigation *in vivo* and in other tissue, particularly in the presence of heat sensitization agents which might be used to lower the therapeutic window as direct validation of phase changes in the lipid bilayer and protein states.

References

1.Taylor BA, et al. Med Phys 2008;35(2):793-803. **2.**Taylor BA, et al. Med Phys 2009;36(3):753-764. **3**.Li C, et al. Magn Reson Med 2009;62(5):1251-1260. **4.**Welch AJ. IEEE Journal of Quantum Electronics 1984;QE-20(12):11. **5.**Henriques FC. Arch Pathol 1947;43:489. **6.** Bischof JC, et al.Biophysical Journal 1995;68(6):2608-2614. **7**.Carpentier A, et al. Neurosurgery 2008;63(1 Suppl 1):21-28 **8**.Young IR, et al. Magn Reson Med 1994;32(3):358-369.